

## Rolling friction on a granular medium

Fabio Vittorio De Blasio<sup>1,2</sup> and May-Britt Saeter<sup>1,\*</sup>

<sup>1</sup>Department of Geosciences, University of Oslo, P.O. Box 1047 Blindern, 0316 Oslo, Norway

<sup>2</sup>International Centre for Geohazards, P.O. Box 3930 Ullevål Stadion, 0806 Oslo, Norway

(Received 11 June 2008; published 12 February 2009)

We present experimental results for the rolling of spheres on a granular bed. We use two sets of glass and steel spheres with varying diameters and a high-speed camera to follow the motion of the spheres. Despite the complex phenomena occurring during the rolling, the results show a friction coefficient nearly independent of the velocity (0.45–0.5 for glass and 0.6–0.65 for steel). It is found that for a given sphere density, the large spheres reach a longer distance, a result that may also help explain the rock sorting along natural stone accumulations at the foot of mountain slopes.

DOI: 10.1103/PhysRevE.79.022301

PACS number(s): 45.70.Mg, 83.80.Fg, 92.40.Ha

### I. INTRODUCTION

It is common experience that wheels meet a high hindrance when rolling on sand. Normally, the coefficient of rolling friction between solid bodies is lower than that of sliding friction [1]. Evidently, sand makes the rolling friction less effective, obliterating the advantage of rolling over sliding. A systematic understanding of rolling friction on a granular medium is still lacking, both theoretically and experimentally. Even the rolling on a solid body has been studied only recently from a theoretical point of view [2]. In comparison, sliding friction on both smooth and irregular surfaces [1,3] and on loose granular media [4] has received much more attention.

There are numerous studies of a sphere rolling along a rugged surface: theoretical [5] and experimental [6,7]. The analysis shows that the repeated collisions of the rolling sphere with irregular bumps (usually obtained experimentally by gluing grains to a tilt table) results in a viscouslike force which depends on the velocity; thus, the velocity of a sphere moving down an inclined plane tends to a constant value. However, to our knowledge the case where the basal granular bed is mobile rather than tied to the sliding plane has been little investigated. Other dissipation mechanisms such as grain-grain friction may play a role when the basal grains are mobile. Moreover, due to the impact with the mobile grains, the latter acquire momentum at the expenses of the sphere, similar to the drag force exerted by a liquid.

The problem of rolling friction on a loose granular medium has also one significant application to the dynamics of taluses—i.e., natural rock heaps at the flank of mountain slopes. Taluses exhibit a longitudinal grading with the largest boulders stopping at the end of the heap [8]. This has been qualitatively explained as the effect of larger momentum carried by the largest stones [8], but a definite physical understanding is lacking. We assume that the movement of a boulder down a talus is akin to the rolling along a loose granular bed. While having this geophysical problem in mind, we maintain a generality of approach, choosing simple systems:

spheres rather than rocky fragments and sand formed by grains of nearly uniform size rather than grains of wide size spectrum like in a natural talus.

### II. EXPERIMENTAL SETUP AND RESULTS

Figure 1 shows the setup used in the experiments. The basic element consists of a flume covered with a thick bed of granular material, along which a sphere is set to roll. The sphere starts from rest and accelerates for a length  $L_0 = 30$  cm on a copper plate before coming across the granular bed. Experimentation shows that the resistance met by the ball increases with the depth of the granular bed until a critical value is reached, where the resistance becomes independent of the depth. The effect is probably similar to the one found in Ref. [9] for the resistance of a sphere falling vertically against the granular material contained in a cylinder. Also in that case the penetration depth of the sphere becomes independent of the thickness of the granular material when the latter is sufficiently thick. By direct experimentation we have found that with the present flume geometry and sand properties, a depth of 14 cm is sufficient to ensure independence of the results with depth. A high-speed camera records the movement of the sphere for further analysis, and a laser precision gauge measures the shape of the groove after the passage of the sphere. Altogether, nine spheres of different diameters have been used: four glass ( $G1-G4$ ) and five steel ( $S1-S5$ ) spheres. Table I gathers the salient material properties of the spheres and sands used in the experiments.

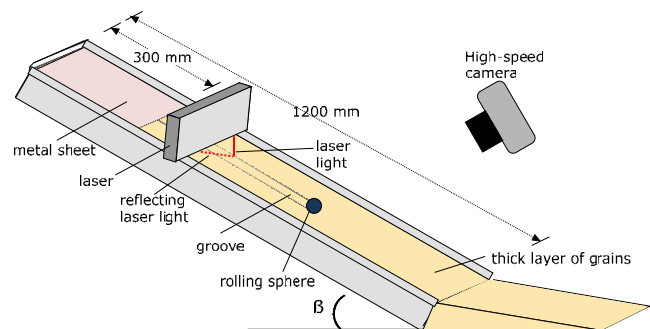


FIG. 1. (Color online) Schematic view of the experimental setup.

\*Present address: Watercourse and Energy Directorate (NVE), Middelthunsgate 29, Oslo, Norway.

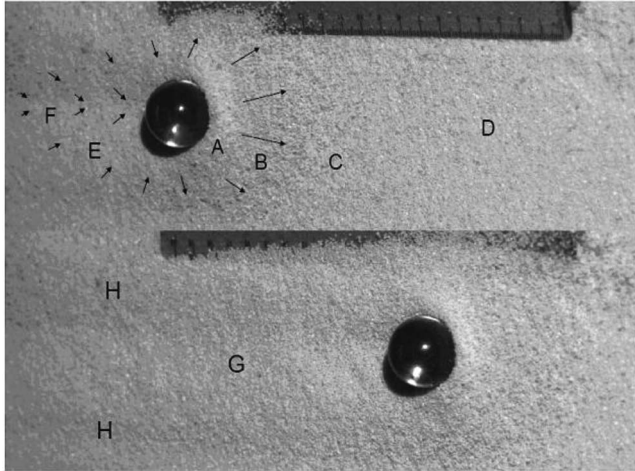


FIG. 2. Two successive snapshots (separated by a time interval of 0.5 s) of the sphere  $G4$  rolling down the bed formed by sand  $A$  at a sloping angle of  $30^\circ$ . The camera was set to a speed of 500 frames per second.

Figure 2 shows a sequence of the glass sphere  $G4$  rolling along the flume. We observed that the area of granular material affected by the sphere is rather wide and long. A compression ridge is created ( $A$  in the figure) embedding a large portion of the sphere surface; this is the region where most of the energy dissipation probably occurs. Sand is pushed at the front forming a blanket that covers the bed surface with a new layer ( $B$ ); several isolated grains are capable of reaching the point  $C$  at relatively high speed. Some out-running grains roll down slope faster, anticipating the arrival of the sphere ( $D$ ). In the region at the two sides of the sphere, the velocity of the granular bed changes direction and points toward the sphere ( $E$ ). After the passage of the sphere, the bed remains

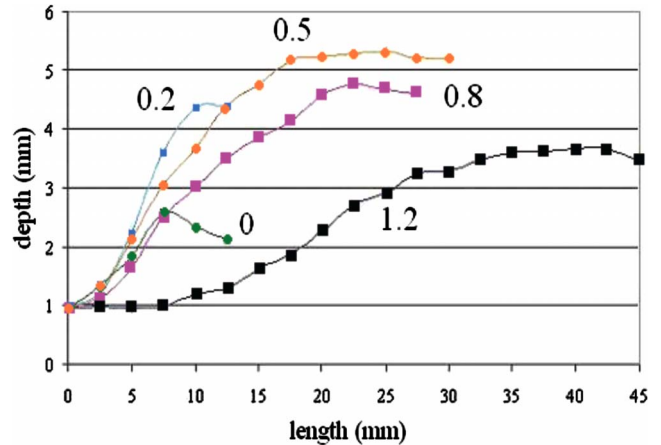


FIG. 3. (Color online) Depth of the groove dug by the large sphere  $G4$  on the sand  $A$  at different velocities measured with laser sensor (AccuRange 600 Laser Displacement Sensor manufactured by Acuity laser measurement).

moderately mobile and follows the movement of the sphere ( $F$ ), partly filling up the groove formed after its passage ( $G$ ). Sand pushed aside forms a groove and a couple of neat and stable levees ( $H$ ).

The structure of the groove left by the sphere was studied with precision laser gauge. Figure 3 shows the results obtained at different speeds of the sphere  $G4$ . At zero speed (static ball resting on the granular bed), the sphere digs a small depression about 1 mm thick and a levee rising about half a mm above the bed. When the sphere is rolling, the groove becomes much deeper—of the order 4 mm—and the distance from the axis of the trajectory affected by reworking increases steadily with the velocity. At the highest of the measured velocities (about 1.2 m/s), the sphere creates a

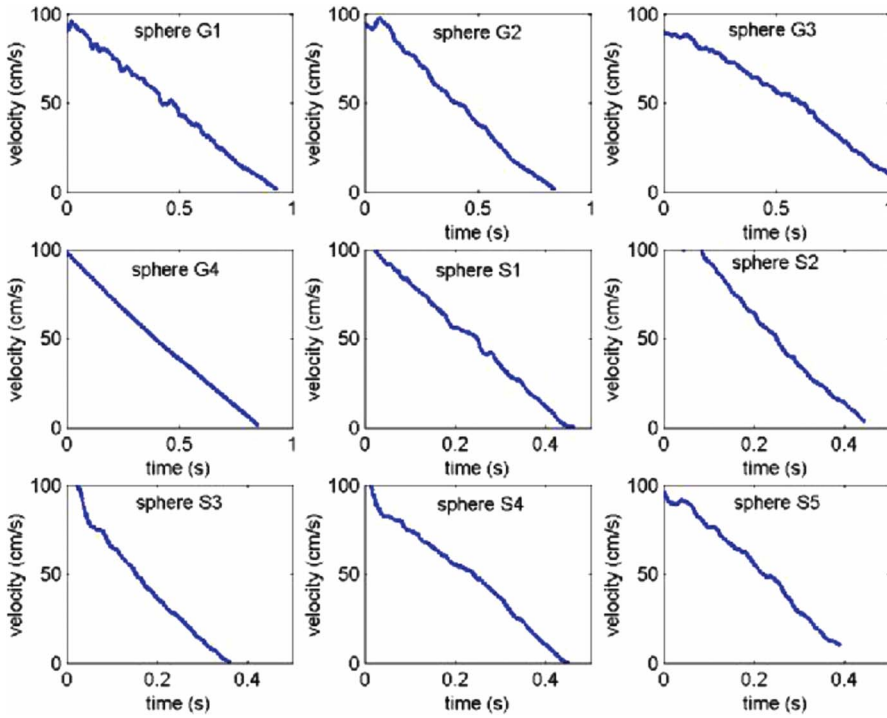


FIG. 4. (Color online) Velocity of the rolling spheres  $G1-G4$  and  $S1-S5$  as a function of time along the path for a slope angle of  $20.5^\circ$ .

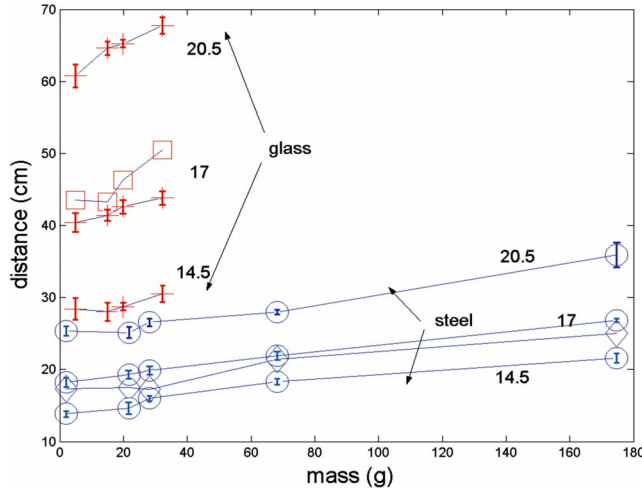


FIG. 5. (Color online) The distance along the flume reached by the spheres as a function of their mass. The numbers refer to the different sloping angles. Crosses and circles: granular medium A. Squares and diamonds: granular medium B. The wide variations in the distance for the same experimental condition required the reiteration of many measurements to lower the standard deviation of the mean (indicated as a bar for each point). The distance reached by the sphere along the flume can be approximately fitted as  $L \approx [0.174 + 4.3 \times 10^{-4} M] \beta^{2.16} \rho^{-0.76}$ , showing strong angle dependence and significant mass and density dependence.

very wide (4–5 cm) but more shallow groove (about 2–3 mm), probably because of the high impact energy. Hence, the volume of the material displaced by the passage of the sphere remains approximately constant at intermediate speeds.

The high-speed movies have been analyzed with the WINANALYZE software (Mikromak Service). Figure 4 reports the results with slope angle of 20.5°. The velocity decreases linearly with time, which implies constant force acting on the sphere. This is surprising, as one might expect the complex dynamics shown in Fig. 2 to generate a velocity-dependent force. Our interpretation of this result is as follows. At low speed, we expect that most of the energy is used up to dis-

place the grains from their rest position. Experiments where a solid cylinder is shifted slowly against a granular bed show that the drag force exerted by the bed is independent of the cylinder velocity and goes like  $\propto kDH^2$ , where  $D$  is the diameter of the cylinder,  $H$  is the depth of the cylinder submerged by the granular bed [10], and  $k \approx 10^4 - 10^5 \text{ N m}^{-3}$ . We obtain a force of the same order of magnitude considering  $H$  and  $D$  as the depth and width of the groove in Fig. 3. For the sphere G4, this gives about 0.01–0.001 N. During its motion, the lower surface of the sphere is embedded in the granular medium (Fig. 2) and is subjected to a force  $\propto RH^2$ , where  $R$  is the sphere radius and  $H$  is the depth reached in the granular medium. Thus the greater resistance on steel spheres is due to their deeper sinking into the granular medium. These results are in marked contrast with the rolling of a sphere on a rigid bumpy plane, where velocity dependence emerges due to the inelastic collisions with the plane [5–7]. Theoretical estimates suggested either a quadratic dependence arising from the continuous inelastic collisions with the irregularities or linear velocity dependence [5]. Experimental investigations indicate a linear law [6].

For our system of loose grains, we expect for higher velocities an acceleration of the form  $dU/dt = A - BU^2$ . This is because upon impact with a single grain of mass  $m$ , the sphere of mass  $M$  changes velocity as  $U' = U/[1 - m(1 + \varepsilon)/(m + M)]$ , where  $\varepsilon$  is the coefficient of restitution. Accounting for the number of grains hit by the sphere per unit time leads to a force contribution of the form  $\propto (1 - v)(1 + \varepsilon)M\rho SU^2/(m + M)$ , where  $v$  is the fraction of voids,  $\rho$  is the bulk density of the granular medium, and  $S$  is the section area spanned by the rolling sphere. The velocity-dependent contribution becomes probably significant at the higher speeds typical of rolling on natural talus slopes.

A constant friction force on the sphere also implies that the motion can be expressed with a friction coefficient  $\mu_{\text{eff}}$ . The determination of  $\mu_{\text{eff}}$  only requires measuring the run-out distance of the sphere, a much simpler procedure than movie analysis, allowing us to carry out numerous measurements (altogether about 1400) and so reduce the experimental errors. The friction coefficient  $\mu_{\text{eff}}$  is found equating the energy reached by the sphere at the beginning of the

TABLE I. Properties of the spheres and of sand used in the experiments.

Spheres	1	2	3	4	5
Mass of the glass spheres (g) $\rho = 2.48 \text{ g cm}^{-3}$	4.94	15.05	19.8	32.24	—
Mass of the steel spheres (g) $\rho = 7.78 \text{ g cm}^{-3}$	2.00	21.70	28.17	68.14	174.71
Denomination of sand used in this work	Commercial name	Origin	Composition	Size	Density (g cm <sup>-3</sup> )
Sand A	Decorative sand	Artificial	Quartz	0.5–1 mm	2.7
Sand B	Rodasand	Natural, sieved river sand	Quartz	0.6 mm	2.7

TABLE II. The effective friction coefficients for the glass spheres.

Angle (deg)	Sphere mass 4.94 g	Sphere mass 15.05 g	Sphere mass 19.8 g	Sphere mass 32.24 g
14.5	0.440	0.443	0.438	0.428
17	0.454	0.450	0.446	0.442
20.5	0.496	0.489	0.488	0.484

granular bed,  $MgL_0 \sin \beta$ , to the potential energy fall in the final position,  $-MgL \sin \beta$  plus the energy dissipated,  $MgL\mu_{eff} \cos \beta$ , where  $L$  is the measured distance reached by the spheres; this yields  $\mu_{eff} = \tan \beta (1 + L_0/L)$ . Figure 5 shows that the distance increases with the mass and decreases with the density of the sphere. Note also the significant dependence on the density and slope angle. The calculated friction coefficient is shown in Tables II and III for the glass and steel spheres respectively. It is found to decrease systematically with the sphere mass and to increase with the slope angle. In addition, the steel spheres show a greater frictional resistance than the glass spheres. Based on an earlier discussion, we interpret this strong density dependence due to marked burrowing of the steel spheres into the medium. The dependence on the sand properties, however, appears less relevant.

The run-out distance and velocity are sensitive to the preparation of the granular bed prior to the experiments. By strictly following the same preparation procedure for all the runs (reworking the granular bed thoroughly and smoothing the surface always in the same manner), it was possible to increase the precision of the results. Henrique *et al.* [7] found a large dispersion of sphere run-out in experiments of rolling on a bumpy incline (some 30% or so). In our experiments, the resistance against the sphere is more similar to a drag force, with particles of the granular bed acting like a medium. Probably because of this, the stopping distance is less dispersed around the mean. The effect is akin to the stoppage of nuclear  $\alpha$  particles in matter, which results in little dispersion of the arrest distance. In contrast, the movement on a bumpy incline as in Ref. [7] is more affected by the random

TABLE III. The effective friction coefficients for the steel spheres.

Angle (deg)	Sphere mass 2.00 g	Sphere mass 21.70 g	Sphere mass 28.17 g	Sphere mass 68.14 g	Sphere mass 174.71 g
14.5	0.631	0.611	0.582	0.541	0.498
17	0.637	0.619	0.609	0.581	0.530
20.5	0.668	0.671	0.654	0.641	0.582

collisions against single grains, as the sphere meets a few of them at a time.

### III. CONCLUSIONS

We found that at velocities  $< 1 \text{ m s}^{-1}$  the rolling friction coefficient is independent of the velocity, which is in marked contrast with rolling on a bumpy incline, but closer to sliding friction. However, in contrast to sliding friction, which is independent of the size of the sliding object, we found that the rolling coefficient decreases with the radius and increases with the density of the sphere. We predict the onset of velocity dependence for greater values of the velocity. When applied to natural stone heaps, the dependence of the rolling friction coefficient on the mass may partly explain the longitudinal sorting effect, whereby the largest boulders are capable of reaching the longest distances. It would be interesting to extend such experiments to larger spheres and higher velocities.

### ACKNOWLEDGMENTS

We thank Professor K.J. Måløy at the Institute of Physics of the Oslo University who generously lent us the high-speed camera and the room for the experiments. We also thank Ken Tore Tallaksen for help with the camera, Ra Cleave of NGI (Oslo), and the technical staff of NGI for aid with other equipment. The software WINANALYZE for the analysis of the sphere motion was kindly provided by Mikromak Service (Berlin, Germany). The paper also benefited from the advice of two anonymous referees.

---

[1] E. Rabinowicz, *Friction and Wear of Materials* (Wiley Interscience, New York, 1995).

[2] N. V. Brilliantov and T. Pöschel, *Europhys. Lett.* **42**, 511 (1998).

[3] B. N. J. Persson, *Sliding Friction: Physical Principles and Applications* (Springer, Berlin, 1998).

[4] S. Nasuno *et al.*, *Phys. Rev. Lett.* **79**, 949 (1997); S. Siavoshi *et al.*, *Phys. Rev. E* **73**, 010301(R) (2006).

[5] E. Wolf *et al.*, *Philos. Mag. B* **77**, 5 (1998); G. G. Batrouni *et al.*, *Phys. Rev. E* **53**, 6496 (1996). S. Dippel *et al.*, *ibid.* **54**, 6845 (1996).

[6] H. M. Jaeger *et al.*, *Europhys. Lett.* **11**, 619 (1990); F. X. Riguide *et al.*, *J. Phys. I* **4**, 261 (1994); F. Radjai *et al.*, *Phys. Rev. E* **52**, 5555 (1995); F. X. Riguide *et al.*, *Europhys. Lett.* **28**, 13 (1994); L. Samson *et al.*, *Chaos* **9**, 639 (1999); L. Samson *et al.*, *Eur. Phys. J. B* **3**, 377 (1998); M. A. Aguirre *et al.*, *Powder Technol.* **92**, 75 (1997).

[7] C. Henrique *et al.*, *Phys. Rev. E* **57**, 4743 (1998).

[8] M. J. Kirkby and I. Statham, *J. Geol.* **83**, 349 (1975).

[9] A. Seguin *et al.*, *Phys. Rev. E* **78**, 010301(R) (2008).

[10] I. Albert *et al.*, *Phys. Rev. E* **64**, 031307 (2001).